Electroencephalographic identifiers of motor adaptation learning

2017 J. Neural Eng. 14 046027

(http://iopscience.iop.org/1741-2552/14/4/046027)

IOP Publishing Journal of Neural Engineering
J. Neural Eng. **14** (2017) 046027 (13pp) https://doi.org/10.1088/1741-2552/aa6abd

Electroencephalographic identifiers of motor adaptation learning

Ozan Özdenizci[1], Mustafa Yalçın[1], Ahmetcan Erdoğan[2], Volkan Patoğlu[1], Moritz Grosse-Wentrup[3] and Müjdat Çetin[1]

[1] Faculty of Engineering and Natural Sciences, Sabancı University, Istanbul, Turkey
[2] Department of Physical Medicine & Rehabilitation, Northwestern University and Rehabilitation Institute of Chicago, Chicago, IL, United States of America
[3] Department of Empirical Inference, Max Planck Institute for Intelligent Systems, Tübingen, Germany

E-mail: oozdenizci@sabanciuniv.edu

Received 28 November 2016, revised 19 March 2017
Accepted for publication 3 April 2017
Published 21 June 2017

Abstract

Objective. Recent brain-computer interface (BCI) assisted stroke rehabilitation protocols tend to focus on sensorimotor activity of the brain. Relying on evidence claiming that a variety of brain rhythms beyond sensorimotor areas are related to the extent of motor deficits, we propose to identify neural correlates of motor learning beyond sensorimotor areas spatially and spectrally for further use in novel BCI-assisted neurorehabilitation settings. *Approach.* Electroencephalographic (EEG) data were recorded from healthy subjects participating in a physical force-field adaptation task involving reaching movements through a robotic handle. EEG activity recorded during rest prior to the experiment and during pre-trial movement preparation was used as features to predict motor adaptation learning performance across subjects. *Main results.* Subjects learned to perform straight movements under the force-field at different adaptation rates. Both resting-state and pre-trial EEG features were predictive of individual adaptation rates with relevance of a broad network of beta activity. Beyond sensorimotor regions, a parieto-occipital cortical component observed across subjects was involved strongly in predictions and a fronto-parietal cortical component showed significant decrease in pre-trial beta-powers for users with higher adaptation rates and increase in pre-trial beta-powers for users with lower adaptation rates. *Significance.* Including sensorimotor areas, a large-scale network of beta activity is presented as predictive of motor learning. Strength of resting-state parieto-occipital beta activity or pre-trial fronto-parietal beta activity can be considered in BCI-assisted stroke rehabilitation protocols with neurofeedback training or volitional control of neural activity for brain-robot interfaces to induce plasticity.

Keywords: motor learning, electroencephalogram, resting-state, pre-trial, brain-computer interface

(Some figures may appear in colour only in the online journal)

1. Introduction

Electroencephalogram (EEG) based brain-computer interfaces (BCIs) are used for direct brain communication in paralysis and motor restoration in stroke [1–3]. Being considered in the context of post-stroke motor rehabilitation, such assistive technology claims to reinforce neural plasticity and support motor recovery [4, 5]. Research in this context focuses on brain sensorimotor rhythm (SMR) activity and exploits such information in a brain-robot interface by rewarding users with movement support by the rehabilitation robot whenever high movement intent is decoded [6–8]. Protocols incorporating such SMR haptic feedback was shown to support modulation of these brain rhythms and enhance post-stroke recovery [9]. Despite this recent progress in BCI-assisted stroke rehabilitation, we believe that the extent of brain activities considered in this context can be a confounding factor for further progress in the field. This argument relies on evidence claiming

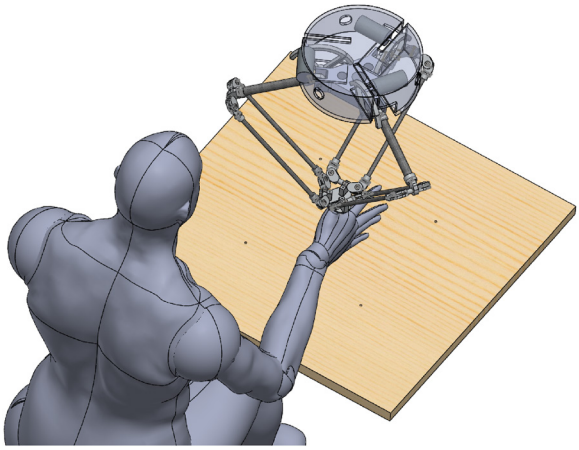

Figure 1. Illustration of the task workspace. Four target locations are placed on the board at the northeast, northwest, southeast, and southwest positions with equal distances of 200 mm from the center.

that a variety of brain activities beyond sensorimotor areas are related to the extent of motor deficits [10, 11]. Furthermore, resembling post-stroke recovery to a form of motor learning [12], various neuroimaging studies showing distinct large-scale networks being involved in different stages of motor skill acquisition also support this argument [13–16]. These findings are consistent with empirical evidence on causal influence of multiple cortical sources on motor learning processes [17]. Thereby, we believe that brain activities beyond sensorimotor areas that are involved in human motor learning should be identified with EEG for potential use in BCI-assisted stroke rehabilitation settings.

In similar contexts, studies investigated how visuomotor learning is reflected in primary sensorimotor areas [18], as well as brain rhythms beyond sensorimotor areas [19–22], during various visuomotor tasks. Generally, such tasks tend not to incorporate physical motor learning, but simply involve fixed motor execution to quantify skill. Moreover, such visuomotor tasks require learning of an underlying mapping between motor task space and visual feedback environment [23], which further incorporates separate processing of different mapping aspects into the learning process [24, 25]. Expectedly, sensorimotor behavior during visuomotor learning was shown to be related with coherence of visual and motor cortex regions [26]. Hence, these studies generally quantify visual mapping performance together with motor execution skill, as visuomotor learning performance.

In previous motor rehabilitation studies, motor learning, which can be evaluated either in the form of motor adaptation or skill learning [27], is widely studied in force-field adaptation tasks [28–30]. In order to dissociate visual mapping from the learning process, we investigate EEG correlates of motor adaptation learning during rest as well as pre-trial movement planning, in the context of a force-field adaptation task without a separate artificial visual feedback environment. The task was performed within an actual physical environment and involved not simply motor execution to quantify skill, but also motor adaptation learning to quantify learning performance.

Based on experimental data from twenty-one healthy participants, EEG correlates of motor adaptation learning were investigated spectrally and spatially during both resting-state and pre-trial phases prior to motor execution. Spectrally, β-oscillations are found to be informative of motor adaptation learning performance. These findings are consistent with evidence in literature suggesting relevance of β-oscillations in mechanisms related to motor maintenance [31–33]. Spatially, a broad network of β-activity was found relevant with a parieto-occipital component beyond sensorimotor regions being involved more strongly in prediction. We further investigated whether changes occur in activities of these EEG correlates with motor adaptation learning and observed a diverse change of pre-trial fronto-parietal β-activity between subjects with higher and lower adaptation rates. Finally we discuss how such EEG identifiers of motor learning can be exploited in future neurorehabilitation settings. A preliminary version of this work was presented in [34].

2. Methods

2.1. Subjects

Twenty-one right-handed healthy subjects (14 male, 7 female; mean age 23.8 ± 3.1) participated in this study. All subjects were naive to the force-field adaptation task. Before the experiments, all participants gave their informed consent after the experimental procedure was explained to them in accordance with guidelines set by the research ethics committee of Sabancı University.

2.2. Experimental setup

The subjects sat in front of a horizontally placed board constructing the task workspace. Subjects were holding a handle, henceforth referred to as an end-effector, with their right hands that was suspended from above onto the board. The end-effector was attached to a 3 degrees-of-freedom modified delta robot which had constrained motion on z-axis [35]. Using the task workspace, the subjects performed the force-field adaptation task (see section 2.3) with simultaneous EEG recordings. The goal of the task was to perform center-out reaching movements under an unknown force-field, as straightly as possible. The end-effector was only capable of two-dimensional movements that were restricted to fall within a circle with a radius of 200 mm. Idle position of the end-effector corresponded to the center of this circle. There were four target locations placed on the circle at the northeast, northwest, southeast, and southwest positions. The target locations were indicated with holes over the board containing LEDs inside. An illustration of the task workspace is provided in figure 1.

2.3. Force-field adaptation task

The force-field adaptation task involved two-dimensional center-out reaching movements (i.e. trials). Goal of the subjects was to follow a straight line path from starting position to the target location. During reaching movements, subjects' motions were disturbed by an external force-field. Within the task workspace, a velocity dependent force-field was

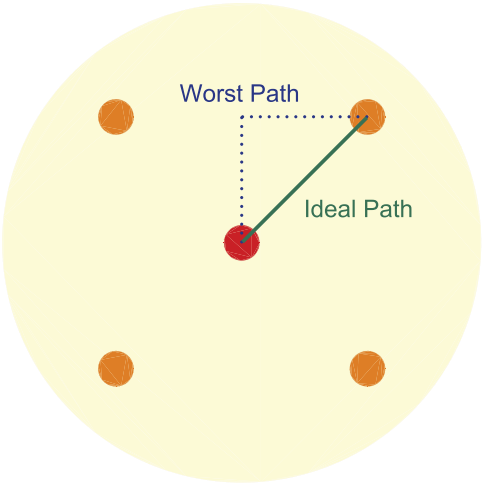

Figure 2. Illustration of the worst center-out movement trajectory for the lower limit *score* of 0 indicated in blue, and the ideal trajectory of a straight line path for the upper limit *score* of 100 indicated in green, assuming the northeast target location is aimed. Red circle at the center represents the starting position and orange circles represent the target locations (200 mm far from the center) with radii of 20 mm.

applied to the end-effector by the robotic setup. Specifically, end-effector velocity vector $\vec{v}$ was multiplied with a constant matrix **B** as in equation (1) at each time point.

$$\vec{f} = \mathbf{B}\vec{v} \tag{1}$$

where **B** was representing the viscosity of the imposed environment and $\vec{f}$ represented the forces that the robotic setup is programmed to produce on the end-effector as the subject performed reaching movements. In particular, **B** was chosen to be

$$\mathbf{B} = \begin{bmatrix} -10.1 & -11.2 \\ -11.2 & 11.1 \end{bmatrix} N \cdot \mathrm{s} \cdot \mathrm{m}^{-1}.$$

The constant matrix **B** was the same as in [36]. During pre-flight and washout phases of the experiment, subjects performed the reaching movements without an external force-field disturbance, but with the same trial flow.

Each trial began with a *planning* phase, where the subjects were instructed to hold the end-effector at the starting position (i.e. center of the circle on the board) and plan the upcoming movement. The *planning* phase lasted 2.5–3.5 s, chosen randomly from a uniform distribution. Within the first second of this phase, the robotic setup guided the subjects to center the end-effector position by directing the end-effector to the pre-calibrated starting position. During the *planning* phase, one of the four possible targets was selected randomly and indicated by a blinking LED light. At the end of the *planning* phase, the LED turned on steadily, signaling the beginning of the *go* phase. The time interval after the first second, until the end of the *planning* phase is referred as the pre-trial phase. In the *go* phase, subjects were instructed to reach for the target by moving the end-effector over the board. A trial was considered complete when the subject moved the end-effector to within 20 mm of the target or if the subject exceeded a time limit of 3 s. After the *go* phase, the subjects were instructed to move the end-effector back to the starting position. At the end of the trials, to quantify motor adaptation amount, a calculated *score* within a range of 0–100 was read out to the subjects through a speaker as an auditory feedback (see section 2.3.1). Each trial began with a new target location.

2.3.1. Auditory feedback score. The *score* in each trial indicated how straight the movement trajectory was in the corresponding trial. To calculate the *score*, we first computed the area between the curve defined by the movement trajectory and a straight line to the target as the kinematic measure [37]. Secondly, this value served as an input variable to a sigmoid function, indicating a gradually diminishing increase [38]. Third, the value of the sigmoid function was multiplied by the elapsed time of the trial as a penalty on the *score*. This encouraged subjects to make faster movements while increasing the effect of the velocity dependent force-field. At the end of each trial, the subjects were informed about their movement performance by inversely mapping this value to a range of 0–100; a higher *score* denoting a faster and more straight reaching movement.

While doing the inverse mapping, to calculate a lower limit for a *score* of 0, the worst movement trajectory was pre-defined as drawing an isosceles right triangle with the straight line to the target being the hypotenuse, in combination with an elapsed time of 3 s. In other words, while calculating the *score* for a particular trial, the initially calculated total area between the curve defined by the movement trajectory and a straight line to the target was proportioned to the area of this pre-defined isosceles right triangle. For an upper limit *score* of 100, the ideal movement trajectory of a straight line path to the target had to be performed. As this was not practically feasible, in order not to prevent the possibility for a *score* of 100 for the subjects, the calculated value after the inverse mapping was rounded to the nearest hundredth (i.e. an inversely mapped value of 99.995 or greater was rounded to 100). Figure 2 illustrates the pre-defined worst and ideal movement trajectories.

Aim of the subjects was to increase their *scores* as close as possible to 100 throughout the experiment, hence attain perfect adaptation to the force-field. No information was provided to the subjects before or during the experiments on how to improve their *scores*.

2.4. Study design

Before conducting the study, to specify an appropriate experiment flow, we executed a demo session with one participant performing the force-field adaptation task for a single target location, which was chosen to be the northeast target location, for a duration of 150 trials. Using the data from this demo session, to be able to gain insights into the neural processes underlying the initial stages of motor learning [13], we investigated an early adaptation time period. Inferred outcomes of this demo session were also used to determine the sufficient length of the experiment.

With the demo session data of 150 trials, exponential fits using nonlinear Nelder–Mead least-squares regression in the

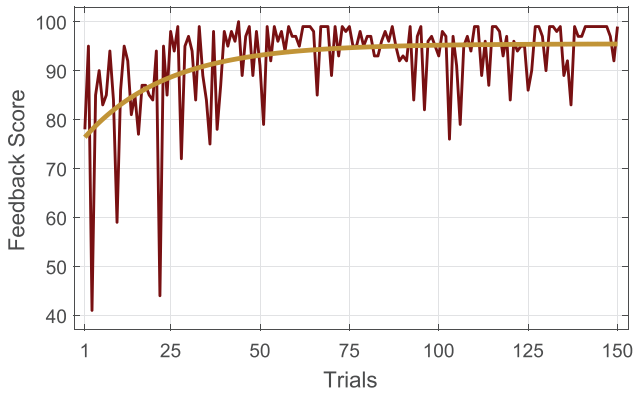

Figure 3. Auditory feedback *scores* of the participant performing the force-field adaptation task for the northeast target location for a duration of 150 trials throughout the demo session. Yellow curve is the exponential fit.

form $S_t = Le^{-t/\tau} + C_{SS}$ were calculated, where S_t is the auditory feedback *score* for trial t, $|L|$ represents the amount of change in *scores*, τ is the time-constant, and C_{SS} represents the steady-state value. The exponential fit solution evaluated values of $S_1 = 76.38$, $S_{40} = 91.90$ and $S_{50} = 93.14$, where the steady-state value was $C_{SS} = S_\infty = 95.47$. Relying on these results, we argue that within the first 40 trials, most but not all of the adaptation was achieved. Figure 3 depicts the changes in auditory feedback *scores* throughout the demo session.

Furthermore, a total of 50 trials was found to be sufficient for learning to reach for a particular target under this force-field and converge performance to a steady-state value. In particular, slope of a univariate linear regression fit to the feedback *scores* was calculated to be very small, indicating no further increase in *scores* (i.e. solutions for $y_t = a \times x_t + b$, where x_t denotes the score at trial t, were obtained as $a = 0.002$ and $b = 94.93$). Therefore, for four target locations, we designed the study for a duration of 200 trials, and approximated to investigate early adaptation during the first 40 trials. Complete study design of the actual experiments is as follows.

All subjects performed a pre-flight phase of eight trials (i.e. eight reaching movements) before the experiments without any force-field to get familiar with the task workspace and trial flow. As part of the force-field adaptation task, each subject performed 200 trials in total, which were divided into three blocks of 40, 80, and 80 trials. Within each of these blocks, there were equal number of trials per target location. After the task, subjects also performed a washout phase of 20 trials which involved no force-field. Alongside the force-field adaptation task, four blocks of resting-state EEG recordings were performed throughout the experiment, each lasting for five minutes. During resting-state recordings, subjects were placed approximately 1.5 m in front of a computer screen and instructed to relax with eyes open, looking at a fixation cross displayed in the middle of the screen. Flow of the experiment is presented in figure 4.

2.5. Data acquisition

Throughout the experiments, the robotic setup recorded data at 500 Hz sampling rate and a 64-channel EEG was recorded at 512 Hz sampling rate, using active EEG electrodes and a BioSemi ActiveTwo amplifier (Biosemi Inc., Amsterdam, The Netherlands). Electrodes were placed according to the 10–20 system. All data were re-referenced to common average reference offline.

2.6. EEG data analysis

Recorded EEG data corresponding to resting-state blocks and pre-trial phases (i.e. time interval after the first second, until the end of the *planning* phase of each trial), which will be used in separate analyses, constituted a large feature space to construct prediction models for motor adaptation learning across a small number of subjects, which was inclined to overfitting. Hence, an informative feature space was obtained by transforming the EEG data into a small number of relevant features. This was achieved by reducing the dimensionality of EEG data both in the spatial and temporal domains.

Specifically for dimensionality reduction in the spatial domain, we pooled all resting-state EEG data from all subjects, by concatenating high pass filtered data at 3 Hz, and separated this data into group-wise statistically independent components (ICs) that represent cortical patterns consistently found across all subjects. This was done by first transforming the data into 64 principal components and then running the SOBI-algorithm, which computes the ICs [39]. We inspected each IC manually and rejected those ICs as non-cortical for which at least one of the following criteria applied [40, 41]: (1) The spectrum did not show the 1/f-behavior typical of a cortical source. (2) The topography did not show a dipolar pattern. (3) The time-series appeared to be contaminated by detectable eye blinks or other noise sources such as 50 Hz line noise. This resulted in remaining six cortical ICs that are later discussed in section 3.2.

For dimensionality reduction in the temporal domain, we transformed EEG data of these ICs into the spectral domain and computed log-bandpowers in four main frequency bands; θ-band (4–7 Hz), α-band (8–14 Hz), β-band (15–30 Hz), and γ-band (55–85 Hz). Specifically, we computed resting-state log-bandpowers of six non-artifactual ICs in four frequency bands of all subjects using an FFT in conjunction with a Hann window spanning the whole five minute resting phase. While computing pre-trial IC-powers, due to varying length of pre-trial duration, FFT was used in conjunction with a Hann window of one second length and a step-size of 100 ms. This analysis resulted in resting-state and pre-trial bandpowers in six ICs and four different frequency bands for each subject, which constituted our final feature space. Subsets of these features in different frequency bands are later used to investigate neural correlates of motor adaptation learning. These features are further analyzed for changes in power during the course of motor learning.

2.7. Motor adaptation learning performance analysis

In order to monitor overall learning effects, four different measures to quantify motor learning performance were investigated; (1) auditory feedback *scores*, (2) total area (*TA*) between the curve defined by the movement trajectory and a straight line to

Figure 4. Flow of the experiment. Before the experiment subjects performed a pre-flight phase. Green blocks indicate five minute resting-state recordings. Red blocks indicate three blocks of force-field adaptation task which in total consisted of 200 trials. Before the fourth resting-state recording, subjects performed a washout phase of 20 trials. Blocks are separated by brief intermissions of one to two minutes.

the target [37], (3) maximum deflection (*MD*) from (i.e. maximum perpendicular distance to) the straight line path to the target during movement [14, 37], (4) coefficient of determination (*r-squared*) between vertical and horizontal movement (i.e. how straight the movement was as an index of skilled movement [42]). On a subject-specific level, these measures constituted a basis for studying individual motor adaptation learning.

Although many studies have used exponential or power law fits of performance data to characterize motor learning, it is known that motor adaptation depends on at least two independent processes with different time scales [43]. Hence, using parameters of exponential or power law fits on performance data across trials may not quantify motor adaptation sufficiently. Moreover, for some individual subject data in our study, exponential fits had r^2 values lower than 0.02 ($p > 0.1$ with a random permutation test with 10^4 iterations). Therefore, individual measures of motor adaptation learning performance variability were calculated under no *a priori* assumptions about the shape of the performance data [44, 45].

Most of the adaptation is observed in the first block of 40 trials where the initial exposure to the force-field took place (see section 3.1). Hence, individual motor adaptation learning performance measures were extracted from that phase of the experiment. As a kinematic measure to quantify motor adaptation, *TA*, which was also used as the basis of auditory feedback *scores*, was utilized after being normalized by scaling to a range of [0, 1] across all subjects. Specifically for each subject, the ratio of average *TA* during first ten trials over average *TA* during the last ten trials of the first block is computed. The resulting ratio, henceforth referred as the motor learning index (MLI), is an adapted version of the learning metric in [14]. The greater the value of MLI, the greater was the observed initial motor adaptation.

2.8. Motor adaptation learning prediction model

Individual MLI measures served as the dependent variables for multivariate linear regression models to predict motor adaptation learning from EEG features. In order to obtain more robust prediction models against outlier variables, we checked all subjects on whether their MLI or any EEG feature exceeded three standard deviations of the median across subjects, as an apriori outlier rejection criterion [46].

2.8.1. Prediction with resting-state EEG features. As part of resting-state prediction, using each subject's six IC powers in one of the four frequency bands from the first resting-state block recorded at the beginning of the experiment as the independent variables, MLI was predicted with a leave-one-subject-out cross-validation protocol. This was done for all frequency bands to investigate if any resting-state neural correlates exist for motor adaptation learning in a particular frequency band.

2.8.2. Prediction with pre-trial EEG features. With a similar approach, MLI was predicted using the information from the first 40 pre-trial IC powers. In particular, slopes of the linear regression fits to pre-trial IC powers in the first 40 trials were used as features. Thus, each subject's rate of change in six IC powers in one of the four frequency bands during the first 40 trials were used as the independent variables to predict MLI. Again, a leave-one-subject-out cross-validation protocol was adopted.

2.8.3. Statistical significance. For both resting-state and pre-trial analyses in each frequency band, to quantify the strength of the prediction model, the correlation coefficient between actual and predicted MLI measures was calculated. Significance of this correlation was tested with a permutation test. To test the null-hypothesis of zero correlation, we randomly permuted the assignment of MLI to features across subjects 10 000 times and estimated the frequency at which the prediction model achieved a higher correlation coefficient than with the true assignment of brain rhythms to performance measures as the p-value.

2.8.4. Feature relevance. In order to gain insights into the neural processes enabling significant prediction, a feature relevance analysis is implemented. We applied multivariate pattern analysis (MVPA) [47] to the EEG data and trained the regression model on all 63 non-empty subsets of the six IC features for all frequency bands. This enables us to identify the most predictive subset of ICs as well as the most significant individual ICs in prediction by interpreting regression weights of the prediction models.

3. Results

3.1. Presence of motor adaptation learning

In the interest of observing the change in movement trajectories as learning proceeds under the force-field, figure 5 shows sample trials for one representative subject from the beginning

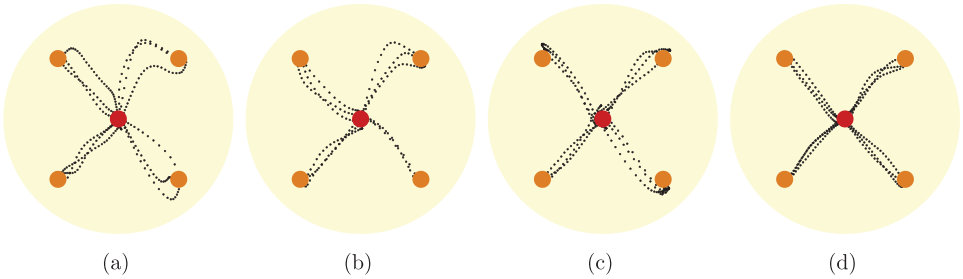

Figure 5. Movement trajectories of one subject during the force-field adaptation task. Three consecutive trials to each target at four different time periods of the experiment are shown; (a) beginning of the first task block, (b) end of the first task block, (c) end of the second task block, (d) end of the third task block. Red circles at the center represent the starting position and orange circles represent the target locations (200 mm far from the center) with radii of 20 mm. Dots are 20 milliseconds apart.

of the first task block, end of the first task block, end of the second task block, and end of the third task block. Visual evaluation reveals that movement trajectories converge to straight line paths by the end of the experiment.

Similarly we examined the after-effects of learning in movement trajectories during the washout trials performed by the end of the experiment under no force-field. Figure 6 shows sample trials for three representative subjects from the beginning and the end of the washout phase. We argue that visual evaluation reveals a re-adaptation in reaching movements recovering from a slight initial irregularity due to the after-effects of learning [36].

From the force-field adaptation task kinematic data, change in performance metrics (*Score*, *TA*, *MD*, *R-Squared*) averaged across all subjects were investigated to observe motor adaptation learning effects. As we are interested in general improvement rather than trial-to-trial changes in performance, 20-trial-averaged performance metrics are plotted (see figure 7). Using the data from these plots, exponential fits using nonlinear Nelder–Mead least-squares regression in the form $M_i = Ae^{-i/\tau} + C$ were calculated, where M_i is the performance measure for trial group i, $|A|$ represents the amount of change in the performance measure due to learning, τ is the time-constant, and C represents the steady-state value. All performance metrics followed a power law with significant correlations between exponential fits and 20-trial averaged metrics; *Score*: $\rho = 0.95$, $p < 10^{-3}$; *TA*: $\rho = 0.73$, $p < 0.03$; *MD* : $\rho = 0.96$, $p < 10^{-3}$; *R-Squared*: $\rho = 0.90$, $p < 0.01$, where p-values are estimated by a random permutation test with 10^4 iterations. Note that, here we do not quantify motor adaptation using any parameter of these exponential fits (as discussed in section 2.7), but only demonstrate that motor learning performance metrics follow a power law as suggested by law of practice [48].

For all measures, strict increase in performance is observed in the first task block (i.e. first two trial groups in figure 7 plots). Moreover, we observe that within the first 40 trials, motor learning performance measures averaged across subjects show significant correlations with one another (see table 1). Hence, we can argue that MLI measures that are extracted from that phase of the experiment can sufficiently quantify motor adaptation learning in our experimental paradigm. Figure 9 shows the distribution of MLI values across subjects, capturing a wide range of motor learning performances.

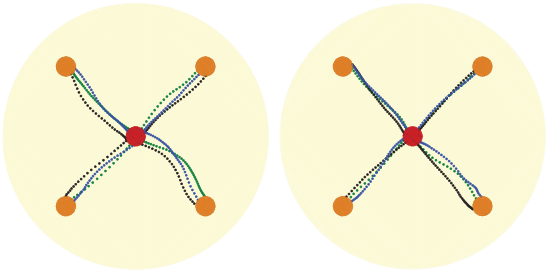

Figure 6. Movement trajectories from three subjects during the washout phase; (a) first trials to each target at the beginning of washout phase, (b) last trials to each target at the end of washout phase. Each different trajectory color represents one subject. Red circles at the center represent the starting position and orange circles represent the target locations (200 mm far from the center) with radii of 20 mm. Dots are 20 milliseconds apart.

3.2. EEG correlates of motor adaptation learning

Six IC topographies resulting from the EEG spatial dimensionality reduction analysis are shown in figure 8. We note that ICs 1 and 4 are likely to represent processes linked to fronto-parietal attention networks [49], IC 2 appears to represent a sub-cortical source, ICs 5, and 6 are generated in sensorimotor cortical areas, and IC 3 appears to represent a parieto-occipital cortical source.

3.2.1. Resting-state analysis. Multivariate linear regression models did not provide statistically significant MLI prediction with θ-, α-, or γ-powers of resting-state EEG features ($p > 0.05$). However, MLI was significantly predicted with resting-state features extracted in β-band ($\rho = 0.54$, $p < 0.02$, see figure 9(b) and table 2). Feature relevance analysis for resting-state EEG prediction yield the subset consisting of IC 2, IC 3, and IC 4 β-powers as the most predictive ($\rho = 0.70$, $p < 10^{-3}$, see figure 9(c)). Significance decreased in comparison to a single β-band prediction, if pairs of frequency bands of the best subset were used as features. For both of these two predictive regression models, the residual plots demonstrated a horizontal band appearance in between two residual standard error levels, indicating the suitability of a linear regression model and absence of potential outliers (see figures 10(a) and (b)).

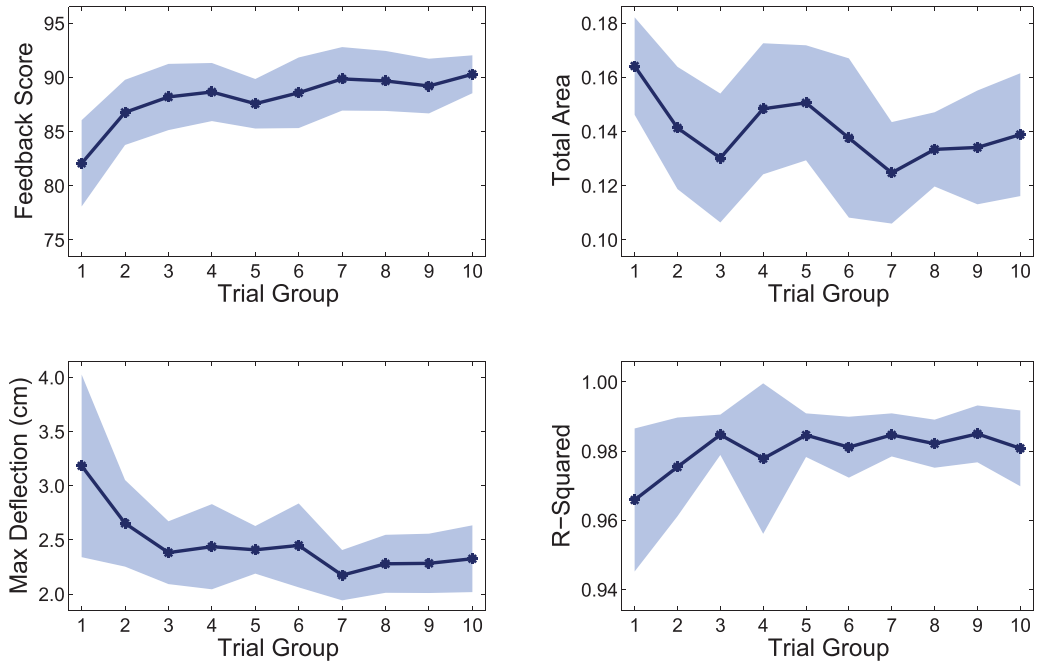

Figure 7. Four motor learning performance measures (*Score*, total area (*TA*), maximum deflection (*MD*), *R-Squared*) averaged over all subjects throughout the experiment. Trial groups represent the sequential order of the 200 trials grouped in 20 trials each. Each point on the blue curve represents an average value over 20 trials. Total area (*TA*) values are normalized to a range of [0, 1] across all subjects and trials before averaging. Shaded regions represent ± one standard deviation of mean measures across the corresponding 20 trials.

3.2.2. Pre-trial analysis. In the case of pre-trial analysis, one of the subjects was discarded due to outlier EEG features across subjects (i.e. rate of change for all IC powers exceeded three standard deviations of the median across subjects). With the remaining 20 subjects' rate of change in IC powers as features, regression analysis did not predict MLI significantly in any frequency band ($p > 0.05$), including the resting-state predictive β-band ($\rho = 0.30$, $p = 0.10$, see table 2). However, feature relevance analysis yields prediction with the subset consisting IC 2, IC 3, and IC 6 β-powers as statistically significant and the most predictive ($\rho = 0.44$, $p < 0.02$, see figure 9(d)). The residual plot for this regression model is shown in figure 10(c), again exhibiting an appropriate horizontal band appearance. For the best subset, again a decrease in significance in comparison to a single β-band prediction was observed, if pairs of frequency bands were used as features. Table 3 shows normalized linear regression weights of each IC for the β-band prediction models, both for resting-state and pre-trial analyses. IC 3, which is likely to represent a parieto-occipital cortical source, has the strongest weight in all prediction models.

As part of the feature relevance analysis, we investigated all non-empty subsets of the six ICs for prediction. However among those, in tables 2 and 3, we have only included the results for the most predictive subset of ICs. In order to explore consistency with existing evidence on relation of sensorimotor activity and motor learning performance, subsets formed by the ICs that represent sensorimotor cortical areas was also observed. The subset consisting of rate of changes in IC 5 and IC 6 β-powers was also found predictive ($\rho = 0.26$, $p < 0.05$).

Table 1. Correlation coefficients between motor learning performance measures (averaged over all subjects) across first 40 trials. p-values are estimated by random permutation tests with 10^4 iterations.

	Score	TA	MD	*R*-squared
Score	1	-0.31^{b}	-0.85^{a}	0.33^{b}
TA	—	1	0.18	-0.31^{b}
MD	—	—	1	-0.50^{a}

[a] $p < 0.01$, [b] $p < 0.05$

3.3. Changes in EEG activity with motor adaptation learning

Over the course of motor adaptation learning, subjects' brain rhythms are likely to show temporary changes. For this reason, both resting-state and pre-trial EEG β-activities that are found to be predictive of motor learning are further analyzed.

3.3.1. Resting-state EEG features. To observe whether resting-state features show an overall change, resting-state β-powers of the six predictive ICs, averaged across subjects as a grand average, were calculated (see figure 11). Difference of grand average β-powers for all six ICs between first and third resting-state recordings (i.e. before the experiment and after force-field adaptation task was completed) were computed and a Wilcoxon signed-rank test was used to test the null hypothesis of zero median. We observed a statistically significant increase in grand average resting-state β-powers of ICs as the force-field adaptation task was completed ($p = 0.03$).

However, resting-state β-powers in none of the ICs significantly changed in a particular direction across subjects. To test this, for each IC, difference of β-powers between first and third resting-state recordings of all subjects were computed

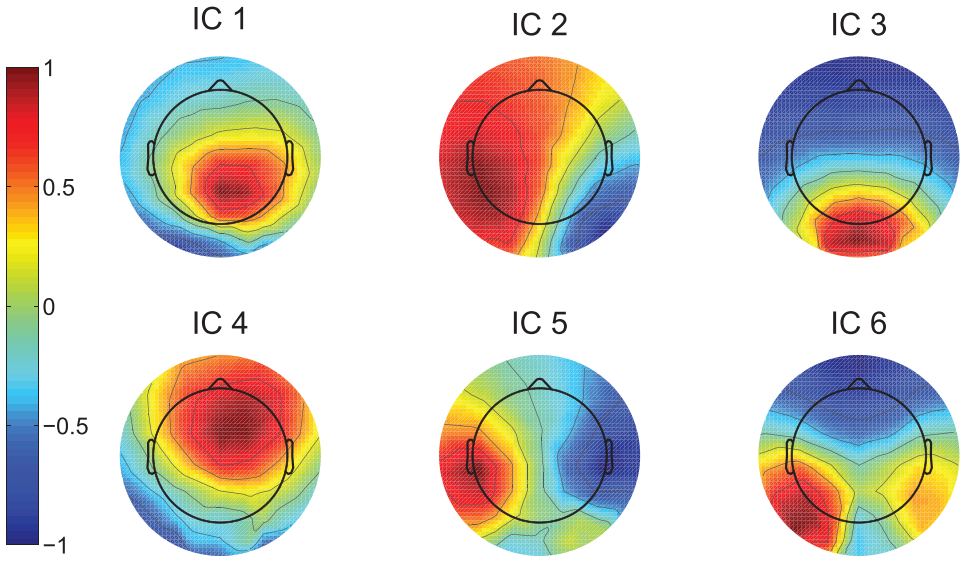

Figure 8. Topographies of the six non-artifactual ICs that represent cortical patterns consistently found across all subjects.

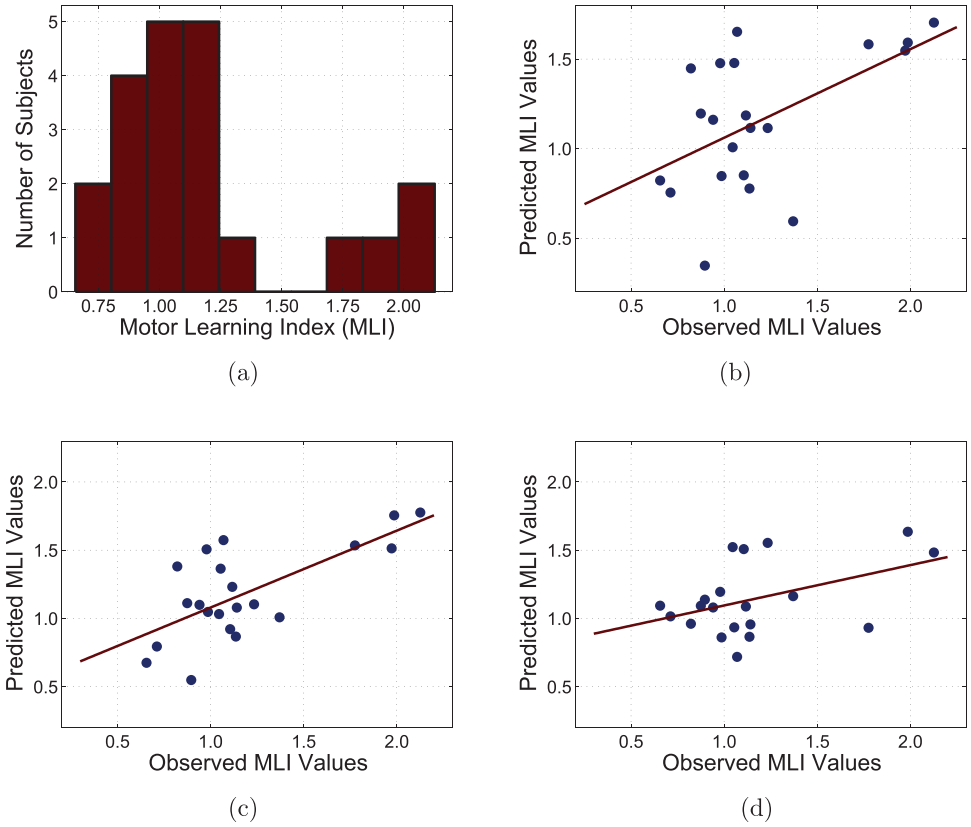

Figure 9. (a) Histogram of MLI measures across subjects. (b) Observed versus predicted MLI using six resting-state IC β-powers as features ($\rho = 0.54$, $p < 0.02$). (c) Observed versus predicted MLI using the most predictive subset of resting-state IC β-powers as features ($\rho = 0.70$, $p < 10^{-3}$). (d) Observed versus predicted MLI using the most predictive subset of rate of changes in IC β-powers during first 40 trials as features ($\rho = 0.44$, $p < 0.02$).

and a Wilcoxon signed-rank test was used to test the null hypothesis of zero median across subjects. No change for individual IC β-powers was observed across subjects through the experiment ($p_{\text{IC1}-6} = \{0.79, 0.25, 0.84, 0.45, 0.76, 0.79\}$).

3.3.2. Pre-trial EEG features. Pre-trial EEG shows rapid trial-to-trial changes in activity. Hence, we investigated two separate groups of subjects that are better representative

Table 2. Correlation coefficients between actual and predicted MLI measures for prediction models in each frequency band when all six IC powers are used as features.

	θ-band	α-band	β-band	γ-band
Resting-state prediction	0.21	−0.07	0.54[a]	−0.53
Pre-trial prediction	−0.01	−0.27	0.30	0.37

[a] $p < 0.02$

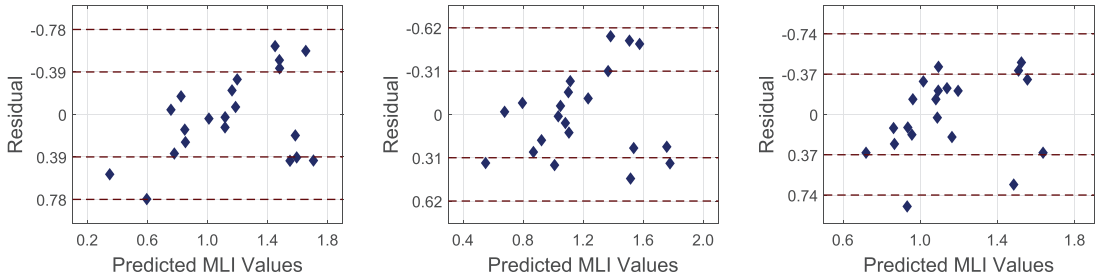

Figure 10. Residuals versus predicted MLI values for regression models with; (a) six resting-state IC β-powers as features (from figure 9(b)), (b) the most predictive subset of resting-state IC β-powers as features (from figure 9(c)), (c) the most predictive subset of rate of changes in IC β-powers during first 40 trials as features (from figure 9(d)). Dashed horizontal lines represent the first two levels of residual standard error.

Table 3. Regression weights for prediction models in β-band averaged over all cross-validation folds. Weights are normalized by dividing by the absolute maximum value.

EEG feature space		Correlation	IC 1	IC 2	IC 3	IC 4	IC 5	IC 6
Resting-state	All ICs	$\rho = 0.54$[a]	0.15	0.21	−1.00	0.71	0.11	0.02
	Best subset	$\rho = 0.70$[b]	—	0.33	−1.00	0.89	—	—
Pre-trial	All ICs	$\rho = 0.30$	−0.43	−0.36	1.00	−0.07	−0.16	−0.61
	Best subset	$\rho = 0.44$[a]	—	−0.59	1.00	—	—	−0.94

[a] $p < 0.02$, [b] $p < 10^{-3}$

of learning with higher adaptation rates (i.e. four subjects with highest MLI measures) and lower adaptation rates (i.e. four subjects with lowest MLI measures). First, pre-trial IC β-powers are averaged within each of these groups. Then for both groups, correlation coefficients between trial indices, ranging from 1 to 40, and group-averaged pre-trial IC β-powers in the first 40 trials were calculated. A random permutation test on the temporal order of trials with 10^4 iterations tested the null-hypothesis of zero correlation. Note that, here a negative correlation coefficient indicates a decrease in pre-trial powers and vice versa.

For IC 5 and IC 6 representing sensorimotor cortical areas, significant decrease in pre-trial powers were observed for the group of subjects with higher adaptation rates; IC 5: $\rho = -0.40$, $p < 0.01$, IC 6: $\rho = -0.40$, $p < 0.01$, which are likely to be caused by stronger β-suppression over sensorimotor cortex as motor learning proceeds [50, 51]. Moreover for IC 4, while a significant decrease in pre-trial powers was observed for the group of subjects with higher adaptation rates ($\rho = -0.32$, $p < 0.02$), a significant increase in pre-trial powers were observed for the group of subjects with lower adaptation rates at the same time ($\rho = 0.36$, $p < 0.02$). For the other ICs and groups, none of the changes in pre-trial powers were found statistically significant.

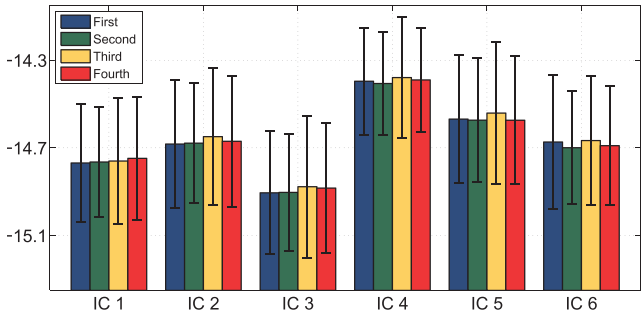

Figure 11. Grand average β-powers of the six ICs over all subjects in four resting-state phases. Error bars indicate $\pm$ one standard deviation across subjects.

4. Discussion

We simulated the post-stroke recovery process of patients in an experimental setup for healthy subjects with a force-field motor adaptation task that involved not only motor execution to quantify skill, but also motor learning to quantify learning performance. Within an actual physical environment, purely focusing on the motor learning process without an underlying visual mapping, subjects learned to adapt to the force-field and generate straight and smooth reaching movements. Motor adaptation rate, as a quantified learning measure, was significantly predicted with EEG features (i.e. resting-state β-powers in cortical ICs and rate of change in these cortical IC powers as adaptation took place) across subjects.

Due to the small number of subject data in comparison to high dimensionality of possible feature spaces (i.e. combinations of frequency bands and cortical sources), we were not able to investigate prediction models incorporating all frequency bands simultaneously. Hence we present all results for individual frequency band features separately and conclude relevance of β-oscillations. We believe that performing a similar series of analysis with more participant data is likely to yield stronger results.

Nevertheless, the observed relation of motor learning and EEG β-activity was found to be consistent with evidence in literature. Motor movements in general have been

associated with changes in prominent β-oscillations [52, 53]. Moreover, event related changes in sensorimotor β-activity were shown to reflect neural processes associated with visuomotor learning [54]. Here we provide empirical evidence that β-activity during rest as well as movement planning before motor execution is related to pure motor learning in general. To date, β-activity was credited as informative of mechanisms related to motor maintenance [31–33]. It has been argued that stronger β-oscillations are observed if maintenance of the current motor status is intended or predicted [31], consistent with the case of Parkinson's disease where patients find it difficult to initiate movements, which is notably associated with higher levels of β-activity [55]. Such evidence further supports reliability of our findings on motor adaptation as a form of a change in current or upcoming sensorimotor state. As participants adapt their movements to the force-field, stronger resting-state β-activity is observed across all predictive ICs as an indicator of maintaining the newly adapted current sensorimotor state.

Different neuroimaging studies provided evidence on existence of resting-state alterations in brain activity with various motor performance tasks [14, 56, 57]. Here we provide evidence that none of the individual ICs are modulated or suppressed across subjects with learning, but they are modulated with learning jointly. Hence, expectedly, same resting-state MLI prediction (as in section 2.8.1) could be performed using IC β-powers from the other resting-state recordings. Using the same regression weights of all ICs for the resting-state predictive model in table 3, MLI can be predicted significantly with features extracted from the second resting-state block ($\rho = 0.56$, $p < 0.02$), third resting-state block ($\rho = 0.62$, $p < 0.01$), or fourth resting-state block ($\rho = 0.43$, $p < 0.05$). This further supports the finding that IC powers across this network are jointly involved in the adaptation process and enhanced or suppressed coherently among themselves. However, whether exploiting resting-state activity of these ICs individually will improve motor learning performance remains an open question.

Recently, using a similar physical force-field adaptation task, cortical re-organizations related to learning were shown to be extended beyond primary motor areas of the brain to sensory systems as well [16]. These observed effects, as decoded from somatosensory evoked potentials, were also shown to be strictly associated with pure motor learning. Here, we further study and identify a broader range of brain activities correlated with motor learning, and coherently claim that the learning-related cortical re-organization is not restricted to primary motor areas only.

Our results on sensorimotor regions (i.e. prediction with and changes in pre-trial activities of IC 5 and IC 6) are consistent with existing evidence on relation of sensorimotor activity and motor learning performance. Beyond that, several other cortical processes are also found to be jointly related with motor learning. This result, as hypothesized, supports the existence of a distributed network of cortical areas being involved in skill acquisition [58]. In particular, prediction of motor adaptation rate is jointly performed with β-powers in sensorimotor areas, fronto-parietal attention networks, and activity in parieto-occipital regions, which had a stronger weight in all prediction models. Fronto-parietal cortical networks are known to be related with visuospatial attention [59, 60]. Similarly, parieto-occipital cortex is linked with visuospatial consciousness in visual attention tasks [61, 62]. In particular within parieto-occipital regions, precuneus is involved in shifting attention between different locations in space [63] and self-consciousness and self-related mental representations during rest [64]. Moreover, there is existing evidence in literature suggesting relevance of the parieto-occipital cortex in motor behavior of monkeys [65, 66], but this was not yet clearly identified with EEG for pure motor learning performance in humans as presented hereby through the predictive nature of parieto-occipital β-activity. Relying on a vast body of evidence broadly linking the parietal cortex with visuomotor control as in visually guided reaching and grasping in physical space [67], we argue that our results on an IC level are not only consistent with existing literature, but also provide a basis on EEG identifiers of pure motor learning that can potentially be studied in the context of post-stroke neurorehabilitation.

We propose different scenarios in order to exploit these EEG correlates of motor learning in future neurorehabilitation settings. Firstly, electrical stimulation of β-activity was considered as an effective technique for neurorehabilitation. Previously, stimulation of β-oscillatory activity in subthalamic nucleus was studied in patients with Parkinson's disease [68]. Similarly, electrical stimulation on primary motor cortex was shown to improve motor evoked potentials [69] and motor adaptation performance [70] in healthy subjects. Likewise, we hypothesize that stimulation of resting β-activity in cortical ICs beyond sensorimotor areas that are found to be relevant for motor learning is likely to improve motor learning performance.

Another favorable approach in the context of BCI-assisted neurorehabilitation would be neurofeedback training of such associative brain areas that are relevant for motor skill acquisition. It has been shown that SMR neurofeedback training improves motor behavior during a reaction-time task [71] or a joystick-based cursor-movement task [72]. Motivated by such pieces of work and the predictive nature of changes in pre-trial IC powers, we hypothesize that a neurofeedback training protocol incorporating pre-trial β-powers in fronto-parietal cortical networks, in particular IC 4, or parieto-occipital β-oscillations (i.e. IC 3) together with SMR activity is likely to improve motor learning performance, possibly in combination with an adaptive training methodology as proposed in [73].

Finally, resembling a neurofeedback training approach, operant conditioning of neural activity for brain-robot interfaces is the ongoing trend in the context of BCI-assisted neurorehabilitation [74]. For these protocols, different brain activities are proposed as features (e.g. slow cortical potentials as proposed in [75], β-band event related desynchronization [76, 77], or sensorimotor rhythms [7, 9]) for brain-machine interfaces that provide operant control of neural activity to induce plasticity and assist motor rehabilitation. Extending the current focus of these studies to a broader range of brain

rhythms, we suggest that results presented in this work should be considered in a similar brain-machine interface setup in further studies. Accordingly, whether these findings can be generalized to stroke patients on an individual level remains as another research problem of interest.

Acknowledgments

This work was partially supported by the Scientific and Technological Research Council of Turkey by a graduate fellowship and under Grant 115M698, and by Sabancı University under Grant IACF-11-00889.

References

[1] Vidal J-J 1973 Toward direct brain-computer communication *Annu. Rev. Biophys. Bioeng.* **2** 157–80
[2] Wolpaw J R, Birbaumer N, McFarland D J, Pfurtscheller G and Vaughan T M 2002 Brain-computer interfaces for communication and control *Clin. Neurophysiol.* **113** 767–91
[3] Birbaumer N and Cohen L G 2007 Brain-computer interfaces: communication and restoration of movement in paralysis *J. Physiol.* **579** 621–36
[4] Daly J J and Wolpaw J R 2008 Brain-computer interfaces in neurological rehabilitation *Lancet Neurol.* **7** 1032–43
[5] Grosse-Wentrup M, Mattia D and Oweiss K 2011 Using brain-computer interfaces to induce neural plasticity and restore function *J. Neural Eng.* **8** 025004
[6] Saraç M, Koyaş E, Erdoğan A, Çetin M and Patoğlu V 2013 Brain computer interface based robotic rehabilitation with online modification of task speed *IEEE Int. Conf. on Rehabilitation Robotics*
[7] Gomez-Rodriguez M, Peters J, Hill J, Schölkopf B, Gharabaghi A and Grosse-Wentrup M 2011 Closing the sensorimotor loop: haptic feedback facilitates decoding of motor imagery *J. Neural Eng.* **8** 036005
[8] Meyer T, Peters J, Brötz D, Zander T O, Schölkopf B, Soekadar S R and Grosse-Wentrup M 2012 A brain-robot interface for studying motor learning after stroke *IEEE/RSJ Int. Conf. on Intelligent Robots and Systems* pp 4078–83
[9] Ramos-Murguialday A *et al* 2013 Brain-machine interface in chronic stroke rehabilitation: a controlled study *Ann. Neurol.* **74** 100–8
[10] Finnigan S P, Walsh M, Rose S E and Chalk J B 2007 Quantitative EEG indices of sub-acute ischaemic stroke correlate with clinical outcomes *Clin. Neurophysiol.* **118** 2525–32
[11] Sharma N, Baron J-C and Rowe J B 2009 Motor imagery after stroke: relating outcome to motor network connectivity *Ann. Neurol.* **66** 604–16
[12] Krakauer J W 2006 Motor learning: its relevance to stroke recovery and neurorehabilitation *Curr. Opin. Neurol.* **19** 84–90
[13] Halsband U and Lange R K 2006 Motor learning in man: a review of functional and clinical studies *J. Physiol. Paris* **99** 414–24
[14] Vahdat S, Darainy M, Milner T E and Ostry D J 2011 Functionally specific changes in resting-state sensorimotor networks after motor learning *J. Neurosci.* **31** 16907–15
[15] Galea J M, Vazquez A, Pasricha N, de Xivry J-J O and Celnik P 2011 Dissociating the roles of the cerebellum and motor cortex during adaptive learning: the motor cortex retains what the cerebellum learns *Cerebral Cortex* **21** 1761–70
[16] Nasir S M, Darainy M and Ostry D J 2013 Sensorimotor adaptation changes the neural coding of somatosensory stimuli *J. Neurophysiol.* **109** 2077–85
[17] Weichwald S, Meyer T, Özdenizci O, Schölkopf B, Ball T and Grosse-Wentrup M 2015 Causal interpretation rules for encoding and decoding models in neuroimaging *NeuroImage* **110** 48–59
[18] Aoki F, Fetz E E, Shupe L, Lettich E and Ojemann G A 2001 Changes in power and coherence of brain activity in human sensorimotor cortex during performance of visuomotor tasks *BioSystems* **63** 89–99
[19] Meyer T, Peters J, Zander T O, Schölkopf B and Grosse-Wentrup M 2014 Predicting motor learning performance from electroencephalographic data *J. NeuroEng. Rehabil.* **11** 24
[20] Wu J, Srinivasan R, Kaur A and Cramer S C 2014 Resting-state cortical connectivity predicts motor skill acquisition *NeuroImage* **91** 84–90
[21] Pitto L, Novakovic V, Basteris A and Sanguineti V 2011 Neural correlates of motor learning and performance in a virtual ball putting task *IEEE Int. Conf. on Rehabilitation Robotics* (IEEE)
[22] Grosse-Wentrup M and Contreras-Vidal J L 2007 The role of the striatum in adaptation learning: a computational model *Biol. Cybern.* **96** 377–88
[23] Sailer U, Flanagan J R and Johansson R S 2005 Eye-hand coordination during learning of a novel visuomotor task *J. Neurosci.* **25** 8833–42
[24] Krakauer J W, Pine Z M, Ghilardi M-F and Ghez C 2000 Learning of visuomotor transformations for vectorial planning of reaching trajectories *J. Neurosci.* **20** 8916–24
[25] Scheidt R A, Conditt M A, Secco E L and Mussa-Ivaldi F A 2005 Interaction of visual and proprioceptive feedback during adaptation of human reaching movements *J. Neurophysiol.* **93** 3200–13
[26] Classen J, Gerloff C, Honda M and Hallett M 1998 Integrative visuomotor behavior is associated with interregionally coherent oscillations in the human brain *J. Neurophysiol.* **79** 1567–73
[27] Krakauer J W and Mazzoni P 2011 Human sensorimotor learning: adaptation, skill, and beyond *Curr. Opin. Neurobiol.* **21** 636–44
[28] Patton J L and Mussa-Ivaldi F A 2004 Robot-assisted adaptive training: custom force fields for teaching movement patterns *IEEE Trans. Biomed. Eng.* **51** 636–46
[29] Gandolfo F, Mussa-Ivaldi F A and Bizzi E 1996 Motor learning by field approximation *Proc. Natl Acad. Sci.* 93 3843–6
[30] Thoroughman K A and Shadmehr R 2000 Learning of action through adaptive combination of motor primitives *Nature* **407** 742–7
[31] Engel A K and Fries P 2010 Beta-band oscillations—signalling the status quo? *Curr. Opin. Neurobiol.* **20** 156–65
[32] Gilbertson T, Lalo E, Doyle L, Di Lazzaro V, Cioni B and Brown P 2005 Existing motor state is favored at the expense of new movement during 13–35 Hz oscillatory synchrony in the human corticospinal system *J. Neurosci.* **25** 7771–9
[33] Brovelli A, Ding M, Ledberg A, Chen Y, Nakamura R and Bressler S L 2004 Beta oscillations in a large-scale sensorimotor cortical network: directional influences revealed by Granger causality *Proc. Natl Acad. Sci. USA* **101** 9849–54
[34] Özdenizci O, Yalçın M, Erdoğan A, Patoğlu V, Grosse-Wentrup M and Çetin M 2016 Resting-state EEG correlates of motor learning performance in a force-field adaptation task *24th Signal Processing and Communications Applications Conf.* (IEEE) pp 2253–6

[35] Ergin M A, Satıcı A C, Patoğlu V 2011 Design optimization, impedance control and characterization of a modified delta robot *2011 IEEE Int. Conf. on Mechatronics* pp 737–42
[36] Shadmehr R and Mussa-Ivaldi F A 1994 Adaptive representation of dynamics during learning of a motor task *J. Neurosci.* **14** 3208–24
[37] Malfait N, Shiller D M and Ostry D J 2002 Transfer of motor learning across arm configurations *J. Neurosci.* **22** 9656–60
[38] Leibowitz N, Baum B, Enden G and Karniel A 2010 The exponential learning equation as a function of successful trials results in sigmoid performance *J. Math. Psychol.* **54** 338–40
[39] Belouchrani A, Abed-Meraim K, Cardoso J-F and Moulines E 1997 A blind source separation technique using second-order statistics *IEEE Trans. Signal Process.* **45** 434–44
[40] Jung T-P, Makeig S, Humphries C, Lee T-W, McKeown M J, Iragui V and Sejnowski T J 2000 Removing electroencephalographic artifacts by blind source separation *Psychophysiology* **37** 163–78
[41] Delorme A, Palmer J, Onton J, Oostenveld R and Makeig S 2012 Independent EEG sources are dipolar *PLoS One* **7** e30135
[42] Lee Y-H, Wu S-K and Liu Y-P 2013 Performance of remote target pointing hand movements in a 3D environment *Hum. Mov. Sci.* **32** 511–26
[43] Smith M A, Ghazizadeh A and Shadmehr R 2006 Interacting adaptive processes with different timescales underlie short-term motor learning *PLoS Biol.* **4** e179
[44] Gordon K E and Ferris D P 2007 Learning to walk with a robotic ankle exoskeleton *J. Biomech.* **40** 2636–44
[45] Kao P-C and Ferris D P 2009 Motor adaptation during dorsiflexion-assisted walking with a powered orthosis *Gait Posture* **29** 230–6
[46] Rousseeuw P J and Leroy A M 2005 *Robust Regression and Outlier Detection* vol 589 (New York: Wiley)
[47] Jimura K and Poldrack R A 2012 Analyses of regional-average activation and multivoxel pattern information tell complementary stories *Neuropsychologia* **50** 544–52
[48] Newell A and Rosenbloom P S 1981 Mechanisms of skill acquisition, the law of practice *Cognitive Skills and Their Acquisition* ed J R Anderson (Englewood Cliffs, NJ: Erlbaum Hillsdale) pp 1–55
[49] Bressler S L and Menon V 2010 Large-scale brain networks in cognition: emerging methods and principles *Trends Cogn. Sci.* **14** 277–90
[50] Pollok B, Latz D, Krause V, Butz M and Schnitzler A 2014 Changes of motor-cortical oscillations associated with motor learning *Neuroscience* **275** 47–53
[51] Kühn A A, Williams D, Kupsch A, Limousin P, Hariz M, Schneider G-H, Yarrow K and Brown P 2004 Event-related beta desynchronization in human subthalamic nucleus correlates with motor performance *Brain* **127** 735–46
[52] Khanna P and Carmena J M 2015 Neural oscillations: beta band activity across motor networks *Curr. Opin. Neurobiol.* **32** 60–7
[53] Davis N J, Tomlinson S P and Morgan H M 2012 The role of beta-frequency neural oscillations in motor control *J. Neurosci.* **32** 403–4
[54] Tan H, Jenkinson N and Brown P 2014 Dynamic neural correlates of motor error monitoring and adaptation during trial-to-trial learning *J. Neurosci.* **34** 5678–88
[55] Schnitzler A and Gross J 2005 Normal and pathological oscillatory communication in the brain *Nat. Rev. Neurosci.* **6** 285–96
[56] Albert N B, Robertson E M and Miall R C 2009 The resting human brain and motor learning *Curr. Biol.* **19** 1023–7
[57] Morin A, Doyon J, Dostie V, Barakat M, Hadj Tahar A, Korman M, Benali H, Karni A, Ungerleider L G and Carrier J 2008 Motor sequence learning increases sleep spindles and fast frequencies in post-training sleep *Sleep* **31** 1149–56
[58] Wander J D, Blakely T, Miller K J, Weaver K E, Johnson L A, Olson J D, Fetz E E, Rao R P N and Ojemann J G 2013 Distributed cortical adaptation during learning of a brain–computer interface task *Proc. Natl Acad. Sci.* **110** 10818–23
[59] Corbetta M 1998 Frontoparietal cortical networks for directing attention and the eye to visual locations: Identical, independent, or overlapping neural systems? *Proc. Natl Acad. Sci.* **95** 831–8
[60] Praamstra P, Boutsen L and Humphreys G W 2005 Frontoparietal control of spatial attention and motor intention in human EEG *J. Neurophysiol.* **94** 764–74
[61] Foxe J J, Simpson G V and Ahlfors S P 1998 Parieto-occipital 10 Hz activity reflects anticipatory state of visual attention mechanisms *NeuroReport* **9** 3929–33
[62] Babiloni C, Vecchio F, Miriello M, Romani G L and Rossini P M 2006 Visuo-spatial consciousness and parieto-occipital areas: a high-resolution EEG study *Cerebral Cortex* **16** 37–46
[63] Wenderoth N, Debaere F, Sunaert S and Swinnen S P 2005 The role of anterior cingulate cortex and precuneus in the coordination of motor behaviour *Eur. J. Neurosci.* **22** 235–46
[64] Cavanna A E and Trimble M R 2006 The precuneus: a review of its functional anatomy and behavioural correlates *Brain* **129** 564–83
[65] Galletti C, Kutz D F, Gamberini M, Breveglieri R and Fattori P 2003 Role of the medial parieto-occipital cortex in the control of reaching and grasping movements *Exp. Brain Res.* **153** 158–70
[66] Fattori P, Breveglieri R, Amoroso K and Galletti C 2004 Evidence for both reaching and grasping activity in the medial parieto-occipital cortex of the macaque *Eur. J. Neurosci.* **20** 2457–66
[67] Culham J C, Cavina-Pratesi C and Singhal A 2006 The role of parietal cortex in visuomotor control: what have we learned from neuroimaging? *Neuropsychologia* **44** 2668–84
[68] Kühn A A *et al* 2008 High-frequency stimulation of the subthalamic nucleus suppresses oscillatory β activity in patients with parkinson's disease in parallel with improvement in motor performance *J. Neurosci.* **28** 6165–73
[69] Feurra M, Bianco G, Santarnecchi E, Del Testa M, Rossi A and Rossi S 2011 Frequency-dependent tuning of the human motor system induced by transcranial oscillatory potentials *J. Neurosci.* **31** 12165–70
[70] Hunter T, Sacco P, Nitsche M A and Turner D L 2009 Modulation of internal model formation during force field-induced motor learning by anodal transcranial direct current stimulation of primary motor cortex *J. Physiol.* **587** 2949–61
[71] Boulay C B, Sarnacki W A, Wolpaw J R and McFarland D J 2011 Trained modulation of sensorimotor rhythms can affect reaction time *Clin. Neurophysiol.* **122** 1820–6
[72] McFarland D J, Sarnacki W A and Wolpaw J R 2015 Effects of training pre-movement sensorimotor rhythms on behavioral performance *J. Neural Eng.* **12** 066021
[73] Özdenizci O, Meyer T, Çetin M and Grosse-Wentrup M 2014 Towards neurofeedback training of associative brain areas for stroke rehabilitation *Proc. of the 6th Int. Brain-Computer Interface Conf.*

[74] Fetz E E 2007 Volitional control of neural activity: implications for brain-computer interfaces *J. Physiol.* **579** 571–9
[75] Yilmaz O, Birbaumer N and Ramos-Murguialday A 2014 Movement related slow cortical potentials in severely paralyzed chronic stroke patients *Frontiers Hum. Neurosci.* **8** 1033
[76] Naros G and Gharabaghi A 2015 Reinforcement learning of self-regulated β-oscillations for motor restoration in chronic stroke *Frontiers Hum. Neurosci.* **9** 391
[77] Naros G, Naros I, Grimm F, Ziemann U and Gharabaghi A 2016 Reinforcement learning of self-regulated sensorimotor β-oscillations improves motor performance *NeuroImage* **134** 142–52